JMEPEG (2000) 9:311-316

Phase Transformation of a CuZnAl Alloy during Friction

Xiaoxia Zhou, Zhengyi Liu, Xiuqin Wei, Yonghong Pan, and Jianpei Zhou

(Submitted 16 June 1998; in revised form 14 November 1999)

Changes in compositions and microstructures in the surface layer of a Cu-Zn-Al shape memory alloy during friction were investigated by means of scanning electron microscopy, electron probe microanalysis (EPMA), X-ray diffraction, and transmission electron microscopy. It has been found that in friction, single M18R martensite β' transforms into $\alpha + \beta$, with the shape and distribution of the new phases varying with the conditions of friction. In mild friction, Zn and Al diffuse over short distances along the sliding direction, resulting in a structure in which needlelike β and α alternate along the sliding surface. In severe friction, where higher surface temperatures and temperature gradients are expected, Zn and Al make long-distance uphill diffusion from inside toward the surface. Consequently, Zn and Al are concentrated on the surface and depleted in the subsurface, and the phase layers present from the outmost surface inward are β, α, $\alpha + \beta$, cross-martensite, and the matrix.

Keywords Cu-Zn-Al alloy, friction, phase transformations, tribology

1. Introduction

According to Ref 1, a white layer, which is ultrafine martensite, forms on the surface of 55SiMnMo steel in sliding. This layer has high hardness up to 1400 kgf/mm^2 and good corrosion resistance, suggested by the fact that after being etched in aqua regia for 5 min, it remains bright white under microscope. It was also pointed out that three requirements must be satisfied for formation of such white layer: (1) thermal shock on the sliding surface, (2) deformation of surface layer, and (3) martensitic transformation. To further understand the nature and conditions for the formation of the white layer, a tribological/microstructural investigation of a CuZnAl shape memory alloy was carried out. In the present work, the original microstructure of CuZnAl before friction was chosen as M18R single martensite β', which is the product of abrupt cooling from elevated temperatures.[2–5] Considering the effect of dynamic recrystallization, an ultrafine martensite microstructure would be expected to form if no diffusion took place during the thermal shock induced by friction. However, both Al and Zn have high diffusivities, and whether they will induce other changes is the question.

2. Experimental Details

A mixture of electrolytic copper (99.995 wt.%), zinc (99.995 wt.%), and aluminum (99.79 wt.%) was melted in air and remelted in a graphite crucible, where the temperature was controlled in the range of 1150 to 1200 °C. The alloy was water quenched immediately after being cast, and then held at 840 °C for 2 h for diffusion annealing. The alloy was peeled before being forged to a 32 mm diameter rod, with the forging temperature in the range of 600 to 800 °C. Chemical analyses showed that the concentrations of Cu, Zn, and Al are, respectively, 70.2, 21.0, and 3.8% by weight. Friction test specimens were then made, which are 15 mm long rings with an external diameter of 28 mm and an internal diameter of 20 mm.

Before each friction test, the specimen was first annealed at 680 °C for 60 min to produce an equilibrium $\alpha + \beta$ dual-phase structure. Results of electronic probe microanalysis (EPMA) of the phases present after the annealing are shown in Table 1. Then a memory training treatment was applied to the specimen. The procedures are as follows:

- annealing at 830 °C for 20 min followed by quenching in water,
- tempering by boiling in 100 °C water for 90 min, and
- stabilizing by repeating the heating/cooling process 0 °C $\rightarrow$ 100 °C $\rightarrow$ 0 °C ten times.

After the treatment, a structure consisting of single-phase martensite β' is formed. Its basic properties were measured and are listed below.

- Microhardness: H_m = 214.5 kgf/mm^2
- Phase transformation points: M_s = 53 °C, M_f = 38 °C, A_s = 42 °C, and A_I = 62 °C

Table 1 Compositions of α and β phases present in the annealed alloy

	Weight percent		
Phase	**Zn**	**Al**	**Cu**
α	24.4	2.9	Bal
β	28.6	4.9	Bal

Xiaoxia Zhou and **Yonghong Pan**, Research Institute, Guangzhou Refrigeration Company, Ltd., Guangzhou 510470, People's Republic of China; **Zhengyi Liu** and **Jianpei Zhou**, Department of Materials Science and Engineering, South China University of Technology, Guangzhou, P.R. China; and **Xiuqin Wei**, Department of Mechanical Engineering, Nanchang University, Nanchang 330029, People's Republic of China. Contact e-mail: lzhou@ncu.edu.cn.

Table 2 Conditions and results of the friction tests

Specimen number	Friction parameters: Speed before loading (rpm), ω	Friction parameters: Pressure (MPa)	Friction parameters: Time (min)	Cooling medium	Results: Speed after loading (rpm), ω'	Results: ω/ω'	Results: Weight loss (g)
112	2000	1.85	15	Oil	1080	0.54	0.01877
113	2000	1.67	15	Oil	1660	0.83	0.01216
114	2000	1.67	15	Water	1280	0.64	0.19135
115	2000	1.85	15	Water	960	0.48	0.13459
116	2000	1.85	3	Water	920	0.46	0.07003
117	2000	1.85	5	Water	940	0.47	0.08390
118	1500	1.85	15	Water	1425	0.95	0.07043

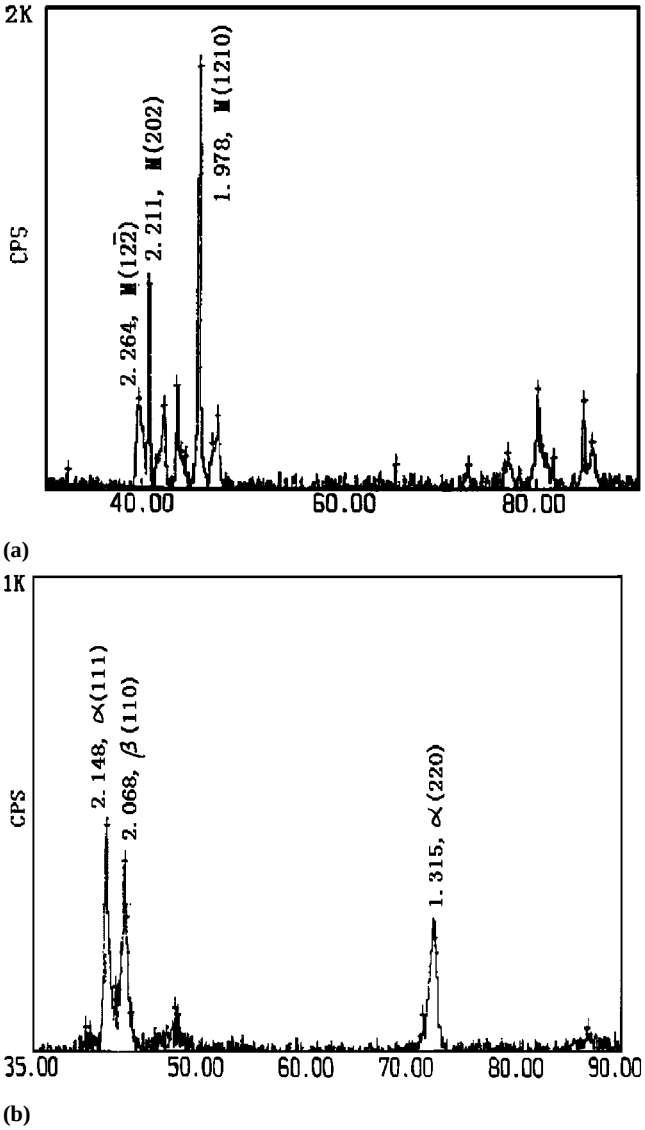

Fig. 1 X-ray diffraction spectra of the CuZnAl alloy specimen 112 (**a**) before friction test and (**b**) after friction test

- Shape recovery rate: $\lambda = 96\%$

The friction tests were carried with a MM-1000 friction tester, which adjusts the sliding rate continuously and the loads

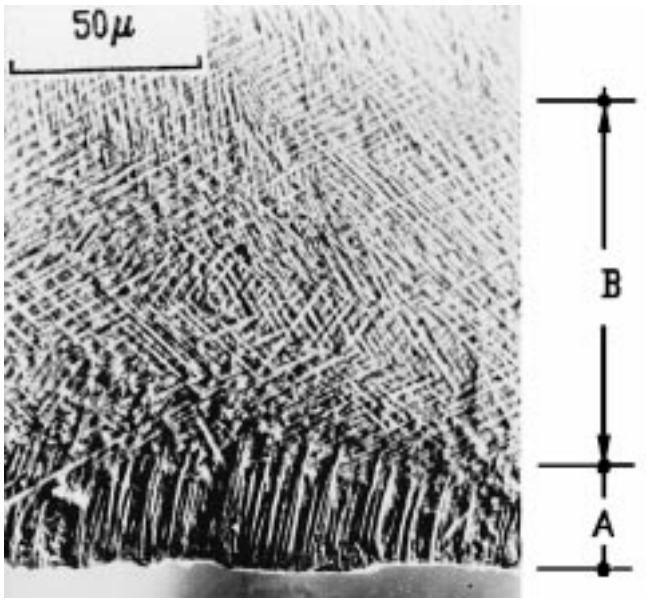

Fig. 2 Cross-section of specimen 112 after friction test (etched in HCL solution with 5% $FeCl_3$, SEM)

pneumatically. The friction couple is made of medium carbon steel (0.45 wt.% C), with its sliding surface induction quenched and 150 °C tempered, reaching a hardness of HRC55-58. The models of the scanning electron microscope (SEM) with electron probe, the transmission electron microscope, and the X-ray diffractometers used are JCX-733, JEM-100CX II, and D/MAX-RC, respectively.

3. Experimental Results

3.1 Friction Conditions and Weight Losses in Friction Tests

Table 2 gives the friction test conditions and the measured results. Before testing, each specimen underwent a run-in procedure of 30 min under 0.98 MPa at 1000 rpm, which ensured an even sliding zone. The cooling media also acts as a lubricant, and it is the great difference in lubricating effect that makes the difference in friction condition.

By comparing sample 112 with 115, and 113 with 114, we found that, with other conditions being the same, the weight

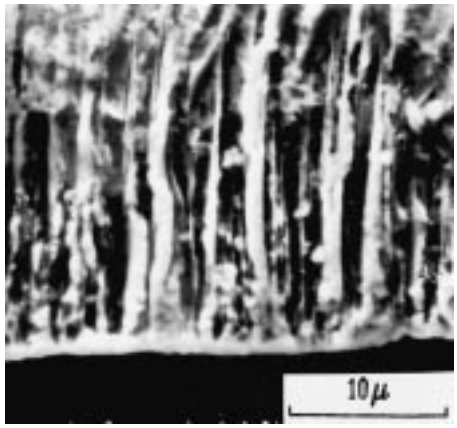

(a)

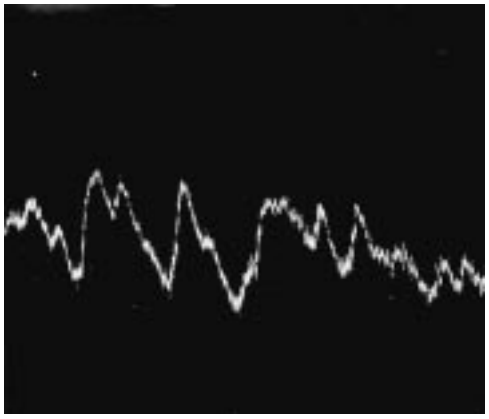

(b)

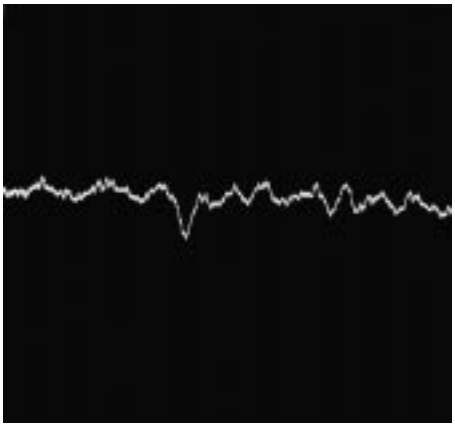

(c)

Fig. 3 A closer view of sublayer A as marked in Fig. 2: (**a**) morphology at higher magnification, (**b**) line scanning profile of Al, and (**c**) line scanning profile of Zn

losses of water-cooled samples are one magnitude higher than those of the oil-cooled ones. Also, the deceleration reduction after loading is larger in the water cooling condition. These facts show that friction under water cooling is more severe than that under oil cooling. The weight loss is fairly independent of conditions other than cooling medium, because in a certain

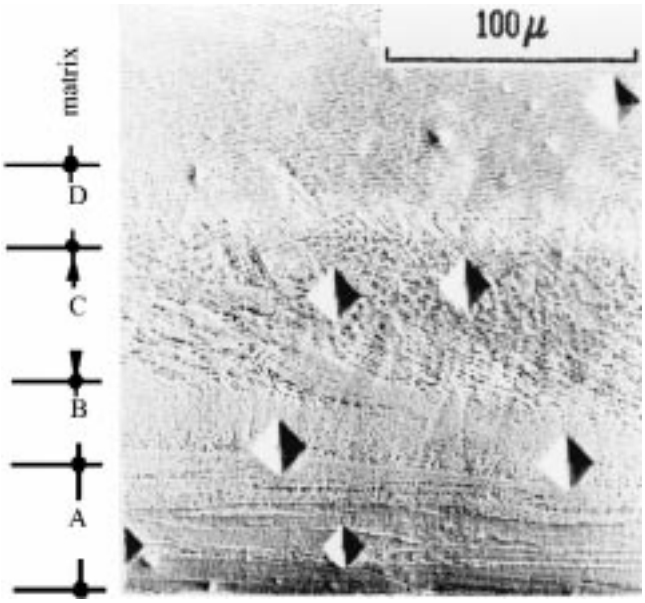

Fig. 4 Cross-section of specimen 115 after friction test and microhardness test (etched in HCL solution with 5% $FeCl_3$, SEM)

range of sliding speed and applied pressure, the cooling condition determines the temperature and temperature gradient of the sliding surface. In the later observation of microstructure and EPMA of compositions, it will be seen that a considerable difference in microstructure results from differences in cooling conditions, which in turn affects wear resistance of the material.

3.2 X-ray Diffraction Spectroscopy

Figure 1(a) indicates that the original microstructure of the alloy before friction test is single M18 martensite β'. Further analysis gives its lattice constants as $a = 0.445$ nm, $b = 0.531$ nm, $c = 3.843$ nm, and $\beta = 89.598°$. The X-ray diffraction spectrum of the post-test specimen, as shown in Fig. 1(b), reveals that transformation from β' to $\alpha + \beta$ occurred in friction.

3.3 Microstructure and EPMA analyses of the friction-affected layer of CuZnAl alloy

For Friction under Oil Cooling (Mild Friction). The cross section of the friction-affected layer of specimen 112 under SEM is shown in Fig. 2. According to the morphology, we divided the layer into two sublayers, marked in Fig. 2 as A and B layers.

Sublayer A is the outmost, with a thickness of approximately 30 μ. It is composed of two phases, α and β. Figure 3(a) shows the morphology of sublayer A at higher magnifications, in which the white strips represent β phase, and the remainders represent matrix α. Figures 3(b) and (c) give the profiles of Al and Zn probed by line scanning across the strips, which supports the above identification. The chemical compositions of the α and β as identified are given in Table 3.

The average hardness of the sublayer A was found to be 252.4 kgf/mm^2. This is not much higher than that of the annealed bulk alloy, which again indicates that the friction under oil

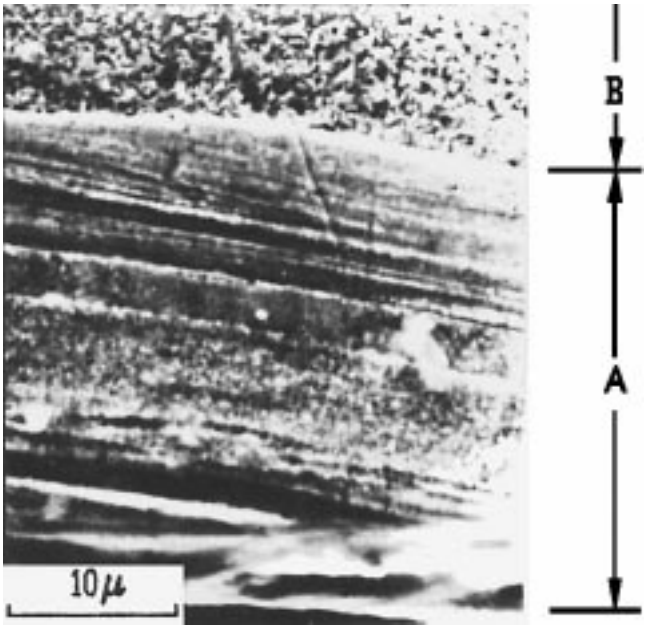

(a)

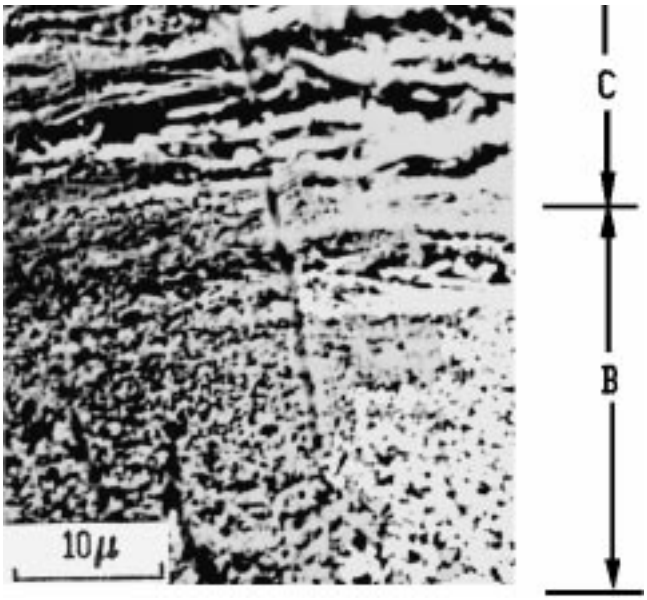

(b)

Fig. 5 A closer view of sublayers A, B, and C, as shown in Fig. 4: (**a**) sublayers A and B and (**b**) sublayers B and C

cooling is really mild, as no significant work hardening of the surface layer occurs.

The B sublayer has a thickness of approximately 100 μ, with the compositions of Al and Zn similar to those of the bulk alloy. Its morphology suggests a structure of cross-martensite, which is characterized by crossed strips.

The fact that the two sublayers have the same average compositions suggests that in the mild friction, Al and Zn only made short-distance diffusion along the sliding surface. Similar structure has been observed in specimen 113, with its sublayers A and B both about one-third thinner.

For friction under water cooling (severe friction). The etched cross section of specimen 115 after friction test and microhardness indentation is shown in Fig. 4. Four sublayers were identified, as marked as A, B, C, and D. The hardness of sublayer A is 479 kgf/mm^2, approximately twice that of the other sublayers. For other water-cooled specimens, only slight differences appeared in thickness and extent of development of these layers. The sublayer D is of crossed-martensite similar to that observed in specimen 112 (Fig. 2). We will focus on the other three sublayers.

Figure 5 shows the sublayers A, B, and C at higher magnifications. It can be seen that the microstructure of A is very fine, with the grain and grain boundaries hardly visible. By contrast, grain and grain boundaries in sublayers B and C are clearly visible, and both layers have hardness similar to that of bulk alloy. The main differences between B and C are that the microstructure of B is finer, with more α than β, while the microstructure of C is coarser with less α than β.

Figure 6 gives the distributions of Al and Zn probed by EPMA and area scan on the cross section of the same specimen. Three bands with varied Al and Zn concentrations from sliding surface inward were revealed, as sequentially marked I, II, and III, with high, low, and modest concentrations of Al and Zn, respectively. Table 4 shows the measured concentrations in each sublayer and the correlation between the sublayers and the bands. We conclude from this result that Al and Zn have made long-distance uphill diffusion from bulk alloy toward the surface, resulting in Al and Zn enrichment in the outermost band and depletion in the inner adjacent band.

From the concentrations of Al and Zn, along with the morphologies, it is deduced that the phase constitutions in the sublayers A, B, C, and D are β, α, $\alpha + \beta$, and cross-martensite, sequentially.

4. Discussion

Segregation of Al and Zn in the friction-affected layer may be caused by the temperature gradient induced vacancy concentration gradient. Equilibrium vacancy concentration C strongly depends on temperature as given by

$$C = A \exp(-Q/\mathrm{R}T)^{[6]}$$

where A and Q are constants. So a strong gradient of vacancy concentration is expected wherever a significant temperature gradient arises. As the sizes of Al and Zn atoms are both larger than that of Cu, they will segregate toward where there are more vacancies.

In a certain range of applied pressure and revolution, the cooling medium is the dominant factor on friction condition. When the cooling medium is oil, the sliding contact is well lubricated and both temperature and temperature gradient are low. So no detectable segregation of Al and Zn toward the

(a)

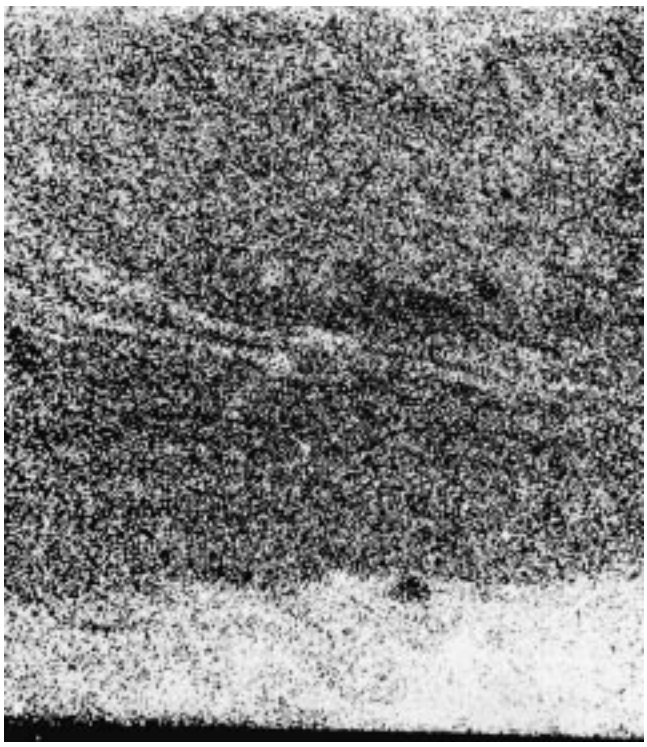

(b)

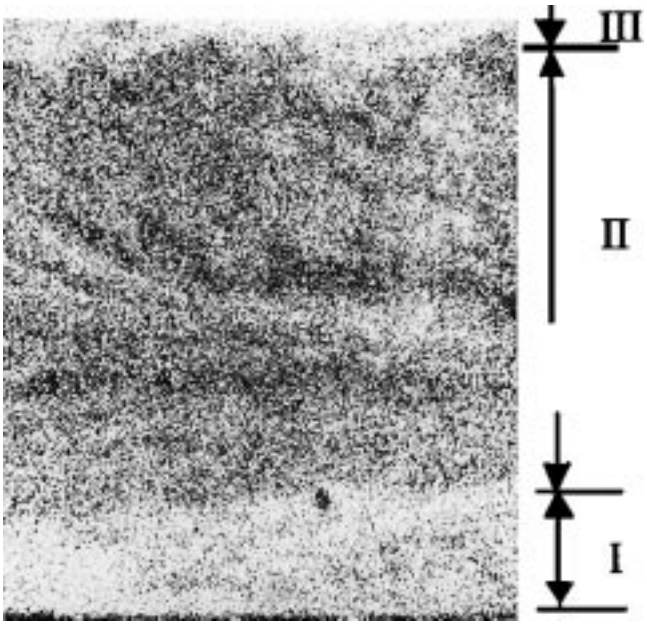

(c)

Fig. 6 SEM and EPMA area scan images of the cross-section of specimen 115 after friction test: (**a**) SEM, (**b**) Al image, and (**c**) Zn image

surface occurred in such a case. In the case of friction test under water cooling, high temperature and temperature gradient results from the severe friction and, hence, significant segregation of Al and Zn toward surface occurred.

5. Conclusions

Phase transformation occurred in the surface layer of single martensite (β') CuZnAl shape memory alloy in sliding friction,

Table 3 Composition of α and β in the sublayer A of specimen 112 after friction test

	Weight percent		
Phase (area)	**Al**	**Zn**	**Cu**
α (dark)	1.5	27.0	Bal
β (white)	4.4	25.6	Bal

Table 4 Chemical compositions in the sublayers of the tested specimen 115

		Weight percent	
Band	**Sublayer**	**Al**	**Zn**
I	A	6.2	24.9
II	B	2.8	21.1
	C	2.9	23.6
III	D	3.4	23.6

and two types of transformation have been identified. In mild friction under oil cooling, two sublayers are formed, with the outer layer consisting of alternate needlelike β and α, and the inner layer being cross martensite. In severe friction under water cooling, Zn and Al make a long-distances uphill diffusion from inside toward the surface, and four sublayers form, with the phases present from the outmost surface inward being β, α, $\alpha + \beta$, cross-martensite, and matrix, subsequently.

References

1. Zhengyi Liu and Jianpei Zhou: *Acta Metall. Sinica*, 1989, vol. 4a, p. 270 (in Chinese)
2. T. Saburi, S. Nenno, and C.M. Wayman: *Proc. 3rd Conf. on Martensite Transformation*, Boston, MA, Trans Tech Publications, Switzerland, 1979, p. 88.
3. S. Sato and K. Takerawa: *Trans. Jpn. Inst. Met., 1968, vol. 9, p. 925.*
4. C.M. Wayman and K. Shimizu: *J. Met. Sci.*, 1972, vol. 6, p. 175.
5. T.A. Schroeder and C.M. Wayman: *Acta Metall.*, 1977, vol. 25, p. 375.
6. J.D. Verhoven: *Fundamentals of Physical Metallurgy*, John Wiley & Sons, New York, NY, 1964.